Design of the Gemini near-infrared spectrograph

Jonathan H. Elias, Richard R. Joyce, Ming Liang, Gary P. Muller, Edward A. Hileman, and James R. George
National Optical Astronomy Observatory, 950 N. Cherry Ave., Tucson, AZ 85719

ABSTRACT

The Gemini Near-Infrared Spectrograph (GNIRS) supports a variety of observing modes over the 1-5 μm wavelength region, matched to the infrared-optimized performance of the Gemini 8-m telescopes. We describe the optical, mechanical, and thermal design of the instrument, with an emphasis on challenging design requirements and how they were met. We also discuss the integration and test procedures used.

Keywords: infrared spectrograph, Gemini telescope, cryogenic

1. INTRODUCTION

The Gemini Near-Infrared Spectrograph (GNIRS) was developed as part of the initial suite of the instruments for the Gemini 8-m telescopes. It was intended to support a range of observing capabilities, matched to the performance of the telescopes[1]. This paper describes the design of GNIRS; a companion paper[2] describes its performance at the telescope.

Previous papers[3,4] described initial concepts for GNIRS. Though the current design is significantly different from these earlier concepts, the capabilities provided remained much the same. The emphasis in this paper is on specific aspects of the design that were particularly successful, and are therefore of general interest.

2. INSTRUMENT REQUIREMENTS

The instrument requirements are summarized below:

- Wavelength coverage from 1-5.5 μm.
- Two pixel scales, of approximately 0.05 and 0.15 arcsec/pixel. The smaller pixel scale was intended both for use in exceptional seeing conditions, and with an adaptive optics system.
- Two spectral resolutions. The lowest spectral resolution was intended to cover a single atmospheric "window" on the detector, which was specified as an ALADDIN 1k x 1k InSb array[5,6]. This implied a resolution ($\lambda/\Delta\lambda$) of ~1700. The second spectral resolution was intended to permit useful work in between atmospheric airglow lines. A resolution of ~6000 was adopted, although higher values were considered.
- A long slit mode of 50 arcsec or greater.
- A polarization analysis mode.
- An integral field unit, which maps a rectangular field onto a long slit or equivalent.
- A cross-dispersed mode, which provides coverage of multiple windows in the R~1700 mode, thus providing complete coverage of 0.8-2.5 μm, though with a short slit.
- A near-infrared on-instrument wave-front sensor (OIWFS), capable of providing guiding and focus referenced to a location close to the instrument input. This was intended as a substitute for the telescope's peripheral wave-front sensors (PWFS). The OIWFS would, in theory, provide better flexure correction and would also provide the ability to work in obscured regions devoid of visible stars suitable for the PWFS.

This list of capabilities implies considerable complexity in the instrument, as indicated schematically in Figure 1, below. The schematic shows only the spectrograph and does not include the OIWFS, which is effectively a parallel "instrument" (see also [6] and [7]).

Ground-based and Airborne Instrumentation for Astronomy, edited by Ian S. McLean, Masanori Iye,
Proc. of SPIE Vol. 6269, 62694C, (2006) · 0277-786X/06/$15 · doi: 10.1117/12.671817

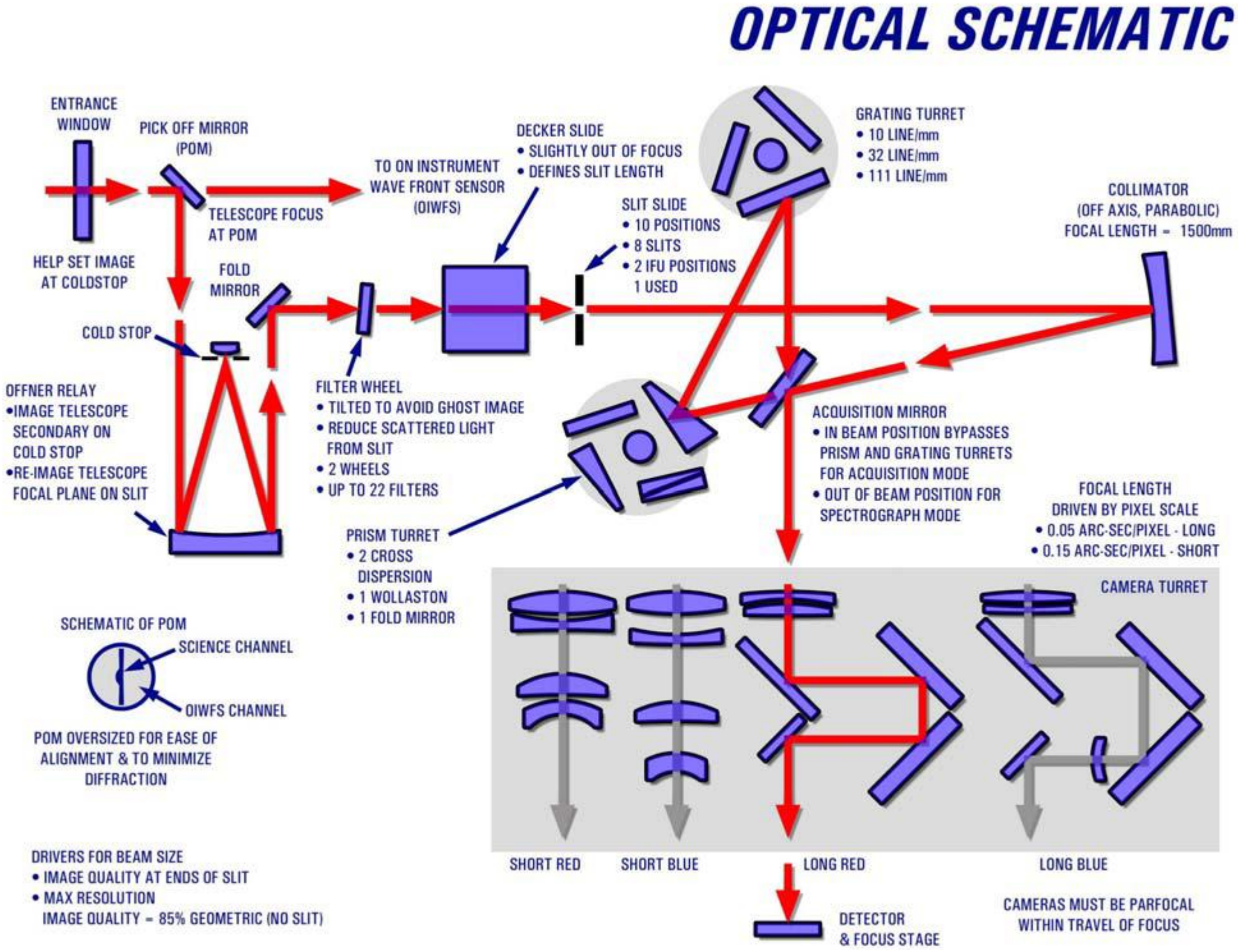

Figure 1. GNIRS optical schematic. Note that everything after the dewar entrance window operates at cryogenic temperatures in order to minimize thermal background radiation.

3. OPTICAL DESIGN

The GNIRS optics can be thought of as divided into two sections:

The fore-optics produce a pupil image (in the case of Gemini, an image of the telescope secondary mirror) at a cold stop, and also re-image the telescope input focal plane on the spectrograph slit. The cold stop is essential to rejecting excess background, and must precede the slit, because some slits are narrow enough that diffraction precludes forming a good pupil image after the slit.

The spectrograph is a relatively conventional spectrograph, though with a variety of configurations to satisfy the requirements outlined above.

3.1 Fore-optics design

The first element in the fore-optics is the dewar entrance window, which is actually a weak lens that serves to put the image of the secondary at an apparent distance of infinity.

The next element is a pick-off mirror, which directs light into the spectrograph from a portion of the field, and allows the remainder of the light to be accessed by the OIWFS. The OIWFS optical design is described in [6] and [7].

After the pick-off mirror comes an Offner relay, which forms an image of the telescope secondary at its secondary mirror. This mirror also defines the instrument's cold stop. Since light is reflected at this point, the area around the secondary must have very low reflectivity to be effective as a stop. Rather than relying on more conventional techniques, such as black paint, we used an optical appliqué, ESLI Vel-Black[8], which has a reflectivity in the infrared of <0.5%.

The blocking filters for the spectrograph are located after the Offner relay, but before the slit. The filters are tilted by 2.7^{o} to minimize ghost images. This location for the filters requires that they all have the same optical thickness in order to avoid focus and position shifts when filters are changed. Most of the filters were fabricated on substrates of 3 mm of BK7, but some longer-wavelength filters were made on higher-index substrates, which were correspondingly thinner.

The Offner structure is 6061 aluminum alloy (see section 4). The Offner mirrors are both diamond-turned, gold-coated aluminum mirrors. The use of an aluminum substrate ensured that the Offner could be aligned at room temperature, and that it would not change focus or alignment when cooled. The mirror surface was diamond-turned on an amorphous aluminum layer deposited on the substrate. The use of an aluminum layer rather than alternatives minimized deformations when cooling while ensuring good optical quality in the machined surface[9]. The flat mirrors are gold-coated mirrors on a fused silica substrate. Although the coefficient of thermal expansion of fused silica is not the same as that of the aluminum structure, alignment is not affected by cooling since the mirror positions are defined using the front surface and lateral motion is acceptable.

3.2 Spectrograph Design

The first element of the spectrograph is the slit. The integral field unit (IFU) is inserted in place of the slit; it acts to slice up a small rectangular field and re-image the slices as a "virtual slit" in the same location as the normal spectrograph slit. The IFU was constructed as a separate unit by the University of Durham (UK); its design and performance are discussed in [10] and [11].

The slit is followed by the collimator. The collimator is an off-axis paraboloid of 1500 mm focal length, operated 4 degrees off-axis. The collimator is another gold-coated, diamond-turned mirror, like the two Offner elements.

Following the collimator is the prism turret, which has four positions. One contains a flat mirror, the second contains an MgF_2 Wollaston prism for polarization analysis, and the remaining two positions contain SF57 Schott glass prisms for near-infrared cross-dispersion, one for each pixel scale. All three prisms have a reflective coating on the back so that they operate in a double-pass mode.

After reflection from the prism turret, light goes to the grating turret. This turret contains three gratings, which provide resolutions of approximately 1700 and 6000 for the two pixel scales, specified in Table 1. The gratings are all blazed for a first-order wavelength of 6.5 μm. This choice generally matches the blaze peaks in higher orders to the centers of the near-infrared atmospheric windows down through 5th order, and allows the use of a single grating to provide efficient coverage over the whole 1-5 μm region. It is true that the use of relatively high orders for the shortest wavelengths does compromise efficiency somewhat. However, if the gratings were limited to use in first or second order only, many more gratings would have been required, resulting in a far larger mechanism. The angle between the incoming and outgoing beams is 27 degrees, which produces anamorphic demagnification of up to ~1.2.

Table 1. Grating parameters

Grating	Lines/mm	Blaze Angle (degrees)	2-Pixel Resolution, long/short camera	Anamorphic Demagnification
1	10.4	2.0	1720/570[a]	1.02
2	31.7	6.2	5150/1750	1.05
3	110.5	22.0	17900/6000	1.22

[a]Configuration underfills detector, not used

Light then goes to the spectrograph cameras. The need to provide two pixel scales required the ability to exchange cameras; we explored a variety of alternative configurations but ended up with separate refractive cameras for the 0.9-2.5 µm region and the 2.8-5.5 µm region, for each pixel scale, for a total of four cameras. The two pixel scales are produced by pairs of cameras which are approximately a factor of three different in focal length; the difference is accommodated by fold mirrors in the long-focus cameras rather than additional optics (see Figures 1 and 3). The camera properties are summarized in Table 2. The materials used are BaF_2, CaF_2 and Schott SF6 glass.

Table 2. Camera parameters

Camera	Focal Length	Number of Elements	Lens Materials
Short "Blue"	435 mm	4 lenses	BaF_2/SF6/BaF_2/BaF_2
Short "Red"	435 mm	4 lenses	BaF_2/CaF_2/BaF_2/BaF_2
Long "Blue"	1305 mm	3 lenses, 4 mirrors	BaF_2/SF6/CaF_2
Long "Red"	1305 mm	2 lenses, 4 mirrors	BaF_2/CaF_2

The most demanding aspect of the optical design is probably the cross-dispersed mode, which requires good focus over a wavelength range of more than an octave. Fortunately, SF6 glass provides very good chromatic correction to BaF_2. The resulting spectrum for the short-focus camera configuration is shown in Figure 2. The spectrum does not use the full array, mainly because the cross-dispersing prism cannot be made larger without producing vignetting.

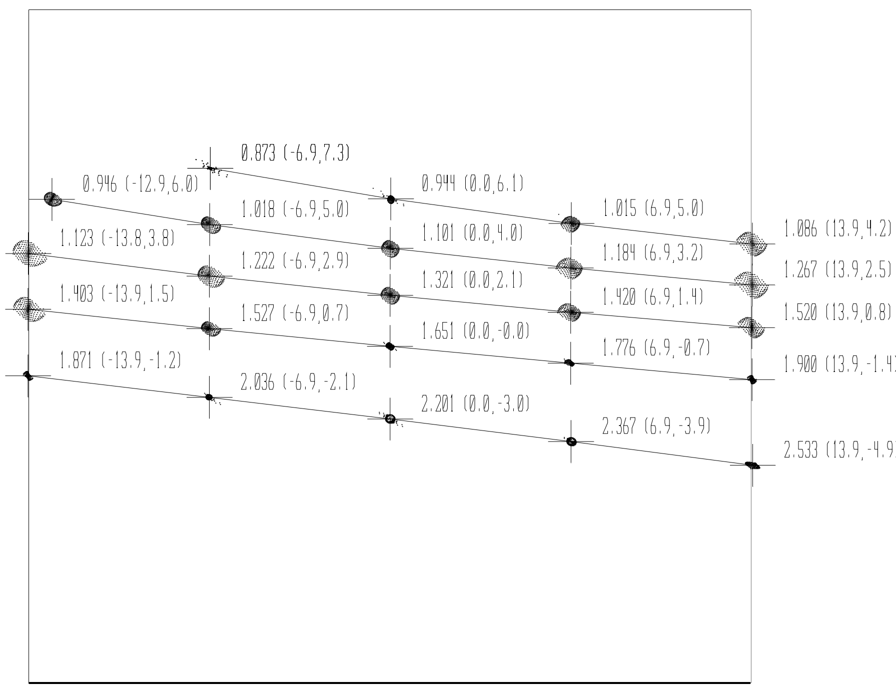

Figure 2. Short-focus camera cross-dispersed mode spectral layout. The grating orders range from 3rd order, covering K band, at the bottom, to 7th order, extending below 1 µm, at the top. The square represents the 1k x 1k ALADDIN array; the spots are enlarged for clarity. The scale for the spots is set by the crosses, which are 27 µm (1 pixel) height and width.

The optical path (see Figure 3 in the next section) allows insertion of a mirror ahead of the prism turret, which sends light directly to the camera. This allows one to view undispersed light in order to acquire science targets; for this purpose the full view of view of the initial pick-off mirror is used. In addition, one of the filter wheel positions contains a small lens, which permits viewing of the cold stop in acquisition mode (this configuration also requires a field lens in the slit slide).

4. MECHANICAL DESIGN

4.1 Overall layout

The location of the spectrograph optics and associated mechanisms within the instrument cold structure ("optical bench") is shown in Figure 3. The light path and optics for the OIWFS are also shown; details have been previously published[5,7] and are not repeated here. The cold structure serves two primary functions: it provides a rigid structure, intended to maintain alignment of the optics under varying gravity, and it also provides a light-tight enclosure, to provent stray light from reaching the detector. Since the InSb detector is sensitive to radiation out to a wavelength of ~5.5 µm, potential sources of stray light include the dewar shell and other room-temperature components. Although the optical bench is enclosed by radiation shields (see section 5) the design does not rely on these shields for protection from stray light. In order to further minimize stray light, the inside of the bench, including baffles, was painted with Aeroglaze Z306 black paint. Mechanisms were black anodized. It was felt to be too risky to paint parts close to the detector, so these were first bead-blasted and then hard black anodized to provide suitable black, diffusing surfaces.

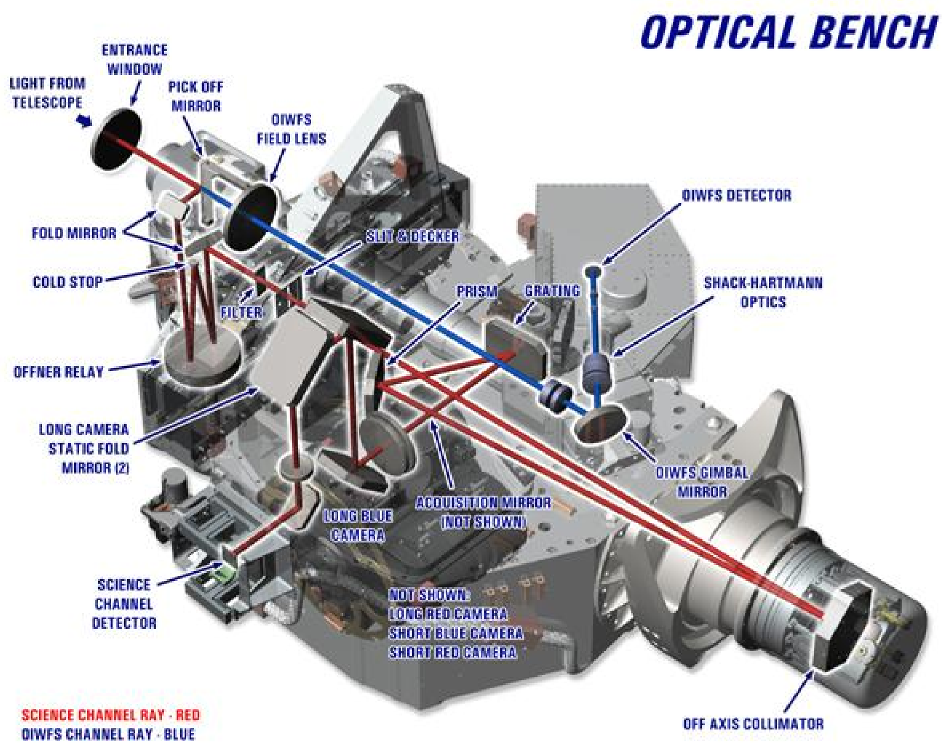

Figure 3. GNIRS optics and mechanisms within instrument cold structure.

Although the optical bench is extremely rigid, there is some flexure, and the mechanisms themselves also display flexure (mainly tilt) under varying gravity. In order to maintain the slit image at a nearly constant location on the detector, an adjustable, passive flexure-compensation mechanism was provided at the collimator mirror. This mechanism tilts the collimator in order to compensate for flexure elsewhere in the optical path; its design has been described in [12]. The bench was attached to the dewar by G-10 trusses. The truss design prevents distortion of the bench when it is cooled and under varying gravity. A similar design is described in [12].

The optical bench is mounted within an approximately cylindrical vacuum vessel, as shown in Figure 4. The overall dimensions are roughly 1.3 m diameter and 2.2 m length. The two enclosures for electronics are mounted on trusses attached to the dewar; the truss dimensions are intended to maintain the overall instrument center of gravity close to the input optical axis, which simplifies installation on the telescope instrument rotator. Ballast weights are used to trim the instrument mass to 2 metric tonnes and adjust the center of gravity to a location 1.0 m from the mounting surface, on the optical axis.

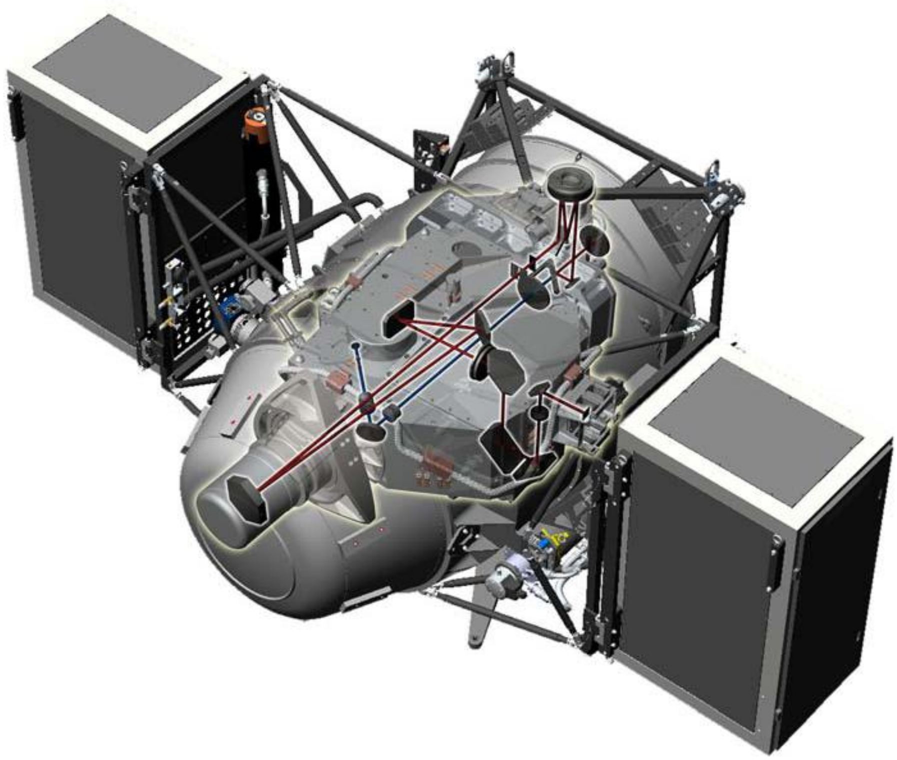

Figure 4. GNIRS dewar with attached electronics enclosures. The mounting truss attaches to the instrument support structure on the telescope. The instrument is shown in the correct orientation for installation on a telescope side port; the optical bench is flipped 180^o from the orientation shown in Figure 3.

4.2 Mechanism design and test

GNIRS contains a total of 9 cryogenic mechanisms in the spectrograph (see Figure 3), in 7 assemblies. Several general principles were followed in the design of all of them:

- All mechanisms were designed to operate at both room temperature and the instrument's operating temperature of ~60 K. This was intended to allow comprehensive testing of mechanism function at room temperature, both prior to integration and as a check on instrument function prior to cooling it.
- All mechanisms were designed to driven by stepper motors and operated "open loop", with a fiducial ("home") position defined by a micro-switch. The one exception to this was the acquisition mirror, which has only two positions, which were both defined by micro-switches.
- All mechanisms were required to operate without interfering with other mechanisms. For mechanisms with a linear range of motion, limit switches were provided.
- Redundant home switches and limit switches were included. The control software allows use of the backup home switches without any manual intervention at the instrument. The back-up limit switches cut power directly to the drive circuitry to ensure that mechanisms with limits cannot be damaged even if the control software is corrupted.
- The mechanisms are all driven by commercial (Phytron) cryogenic motors, which are mounted externally to the light-tight volume defined by the optical bench. The mechanism drives pass through the wall of the bench and are appropriately baffled. This arrangement prevents light (thermal radiation) from the motors from reaching the detector. The motors are thermally isolated from the bench as well (see section 5).

- Ball bearings were used on all shafts and axles. Although we initially intended to use bearings lubricated in-house with MoS_2 dry lubricant, these showed durability problems and we ended up using commercial ball bearings with vacuum-deposited MoS_2 for most of the mechanism drive trains.
- Where possible, existing designs or design concepts were adopted.

During fabrication and integration, each mechanism assembly went through a series of tests:

- Initial shop assembly. This was essentially a fit check, but in principle served as well as a basic functional check.
- Warm test after cleaning. The mechanism parts were all cleaned for cryogenic operation. Dry lubricant (MoS_2) was applied as appropriate. The mechanisms were then operated manually in this clean condition, and drive torques were directly measured. Some flexure testing was also carried out. This was done by mounting the mechanism securely and applying forces through the center of gravity while measuring deflections at relevant locations (e.g., ends of axles). This clean test step was essential, in that it identified many problems that were not apparent in the initial fit check, and which would have been difficult to diagnose during subsequent cold tests. Thorough cleaning of the mechanism parts ensured that the warm behavior of the mechanisms approximated the cryogenic behavior.
- Cold test in test dewar. Once the mechanisms passed the warm tests, they were tested individually in a large test dewar. The test dewar was cooled by liquid nitrogen, so the tests were done at ~85 K rather than the GNIRS operating temperature of ~60 K. The cold tests included repeatability checks using the "home" switches and extended operation (~24 hours continuous).

These test procedures ensured that nearly all mechanism problems were identified prior to integration into the instrument; the warm tests in particular allowed rapid diagnosis. Table 3 summarizes the test phase where problems were identified. The problems identified during the initial warm test are only those that required a modification of the mechanism, and do not include minor rework that one would think of as “fit checking.”

Table 3. Subsystem test results summary

Test Phase	Problems Identified
Initial warm test	2
Clean warm test	5
Cold test in test dewar	3
Integration and test	2

The majority of the problems were identified prior to cold test, and almost all were identified prior to integration into the instrument.

4.3 Mechanism details

Although some of the mechanisms were relatively simple (e.g., the filter wheels), others were not. We discuss the design of the three turret mechanisms, and provide a more limited discussion of the slit mechanism (which also carries the IFU), the detector focus stage, and optics mounts.

4.3.1 Turret design

The three turrets all had similar functionality, and therefore a common design concept was used for all three. The requirement was to accurately position one of 3-4 optical elements with a mechanism of adequate stiffness (both warm and cold). The design was required to work with a total moving mass of ~70 kg, which was our initial, conservative estimate for the camera turret mass (the actual mechanism was approximately 50 kg).

The turret axle design used modified tapered roller bearings at each end (see Figure 5), with a tapered collet and spring maintaining stiffness while allowing for differential contraction during between the warm and cold state, and during cooling and warming.

In principle, this mechanism is very stiff, but we found that in practice there could be excess flexure, which proved to be due to mismatches in the conical surfaces defined by the inside of the turret hub (Figure 5, top right) and the outside of the bearing race (Figure 5, middle right). Careful matching of these surfaces and increasing the pre-load spring force minimized the problem.

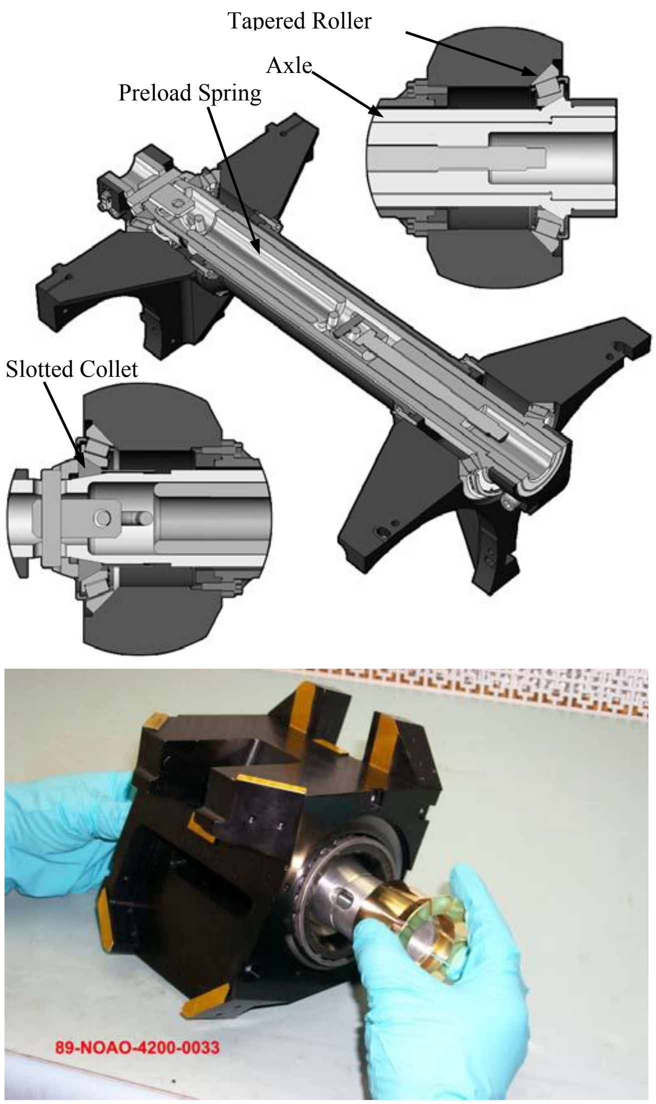

Figure 5. Turret axle design and assembly. The axle concept (upper left) is for the camera turret; the parts and assembly shown to the right and lower left are for the prism turret. The primary differences between individual turrets are the axle length and the spring force, which is matched to the turret mass.

4.3.2 Slit slide

The slit slide proved to be the single most demanding mechanism in the instrument. This is because this mechanism was required to carry the slit mask and two integral field units[10,11], each of which was specified as having a mass of 1 kg.

(Since only a single IFU was built, the actual mechanism has a dummy weight in lieu of the second IFU.) This requirement led to a linear motion with almost 10^6 motor steps to cover the needed range of motion. The slide was supported on crossed roller bearings, loaded by a parallel flexure (see Figure 6). The drive mechanism was a half-nut attached to the slide and driven by a split, spring-loaded worm. The overall mass of the slide was approximately 10 kg, and a counterweight of the same mass is provided to limit forces on the drive.

Figure 6. Front of slit slide, showing slit and IFU carrier (top, left) and counterweight (bottom, left). The drive is shown (right) with the slide removed. The picture shows dummy IFU units; see [11].

Although the desired precision of motion was ~1 μm, in practice the repeatability achieved is ~10 μm; this has little practical impact on operation[2].

4.3.3 Focus stage

The focus stage consists of two sets of parallel flexures on either side of the detector. The spring force in the flexures is sufficient to load the assembly against gravity in all orientations, over the full focus range. The focus motion is driven by parallel cams, which are linked and act against both sets of flexures. This arrangement provides a very precise and repeatable focus motion; tilts induced by the motion or by gravity are acceptably small (less than 25 μm across the detector). The cam drive effectively makes this a rotary mechanism as opposed to a linear drive, so no limit switches are required.

4.3.4 Lens mounts

With the exception of the small pupil-viewing lenses, only the four cameras contain refractive optics. The short-focus cameras contain the largest lenses, and also have the tightest alignment requirements. We also needed lens mounts that were relatively compact, given the need to fit four cameras into a turret.

Figure 7. Camera barrel parts (left) and assembly (right). The left-hand picture shows the front half of a camera barrel showing hard points and two axial rings. The right-hand panel shows part of the assembled camera. Note the springs applying the axial forces and the housings for the radial spring plungers (on left side of barrel).

We adopted a 3-point radial and axial mount, illustrated in Figure 7, above. The 3 axial points are machined in the camera barrels, with axial forces provided by a spring-loaded ring. The radial supports consist of 2 hard points and a spring-loaded third point. A layer of Kapton tape is placed at all hard points to reduce friction and decrease thermal stresses.

5. THERMAL DESIGN

The GNIRS cooling system was required to meet a variety of requirements:

- Rapid cool-down and warm-up; initially specified as 48 and 24 hours respectively, though later relaxed.
- Operation on the telescope with no liquid cryogens.
- Maintenance of stable structure and detector temperatures.

The design that was adopted relies on four Leybold 5/100 GM cold-heads for primary cooling. These are supplemented by a liquid nitrogen pre-cool system.

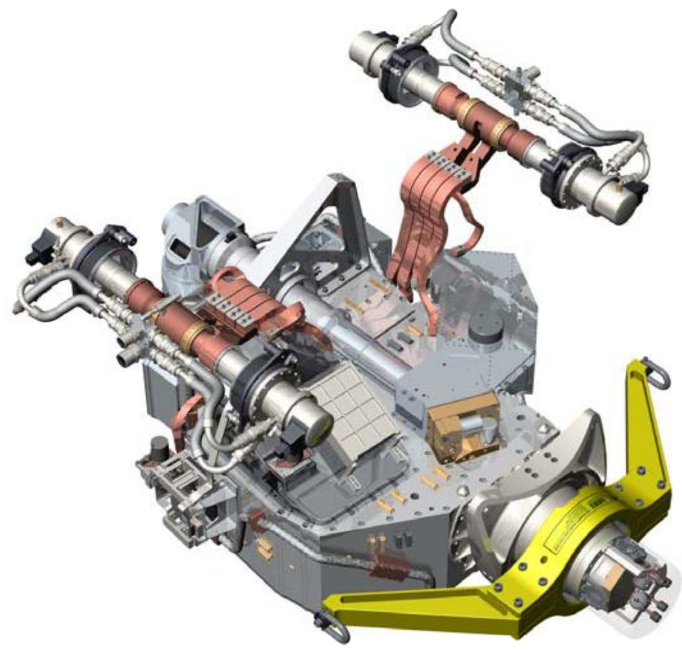

Figure 8. Connections between the cryo-coolers and the optical bench. The cold strap to the science detector is also shown (to left of the optical bench, above focus stage), as are the straps to the active shield. The shields are not shown. The yellow fixture on the lower right is a handling fixture.

The dominant source of heat flow into the cold structure is radiation, which is reduced to ~100 W by two passive shields made out of sheet aluminum. The radiation from the innermost passive shield is intercepted by a third, "active" shield, which is connected to the cryo-coolers and which is thermally isolated from the optical bench (except for the indirect connections through the cold straps). The design ensures that there is very little radiated heat input directly into the optical bench structure; additional heat inputs include radiation through the dewar window into the OIWFS patrol field, conduction through the G-10 supports for the optical bench and through wiring to the bench, and heat generated by the motors. Note that the motors are strapped to the active shield (see 4.2 above) and therefore heat inputs to the bench from mechanism operation are minimized.

The pre-cool system is a simple design that enables distributed cooling of the structure. It consists of corrugated stainless steel tubing which is clamped to the structure at various points (see Figures 8 and 9). Liquid nitrogen flows into the tube and evaporates as it passes along the system. The flow is adjusted to the maximum that will fully evaporate the liquid flowing into the system. Since the dewar is under vacuum all cooling takes place through the points where the tube is clamped to the bench; the cooling produced at the attachment points was measured using a prototype system and the number of attachment points was then specified to result in a cooling rate of 10 K/hour, which was considered to be a safe rate for the refractive optics.

The pre-cool system becomes inefficient once the structure temperature gets close to 80 K, and further cooling to the operating temperature of 60 K must be accomplished using the cryo-coolers only. The pre-cool system is backfilled with helium gas and valved off; this procedure minimizes the risk of developing an ice plug inside the pre-cool system during operation of the instrument, which is normally maintained cold for many months at a time.

The pre-cool system can cool the internal structure to ~80 K in less than 30 hours if it is operated at maximum efficiency; the cryo-coolers can then cool the structure to ~60 K in less than 20 hours.

In order to warm up the structure rapidly, a network of 48 power resistors is distributed over the structure (see Figures 8 and 9). These are divided into 6 parallel circuits to provide redundancy. The heating circuit is capable of dissipating ~2.5 kW into the structure. Continuous operation at this power level would result in warming up the structure much faster than the allowed limit of 10 K/hour, especially at low temperatures, where the specific heat of aluminum is less. The structure temperature is therefore monitored and a temperature controller is used in a "ramp" mode to warm up at 10 K/hour, for a warm-up time of somewhat longer than 24 hours.

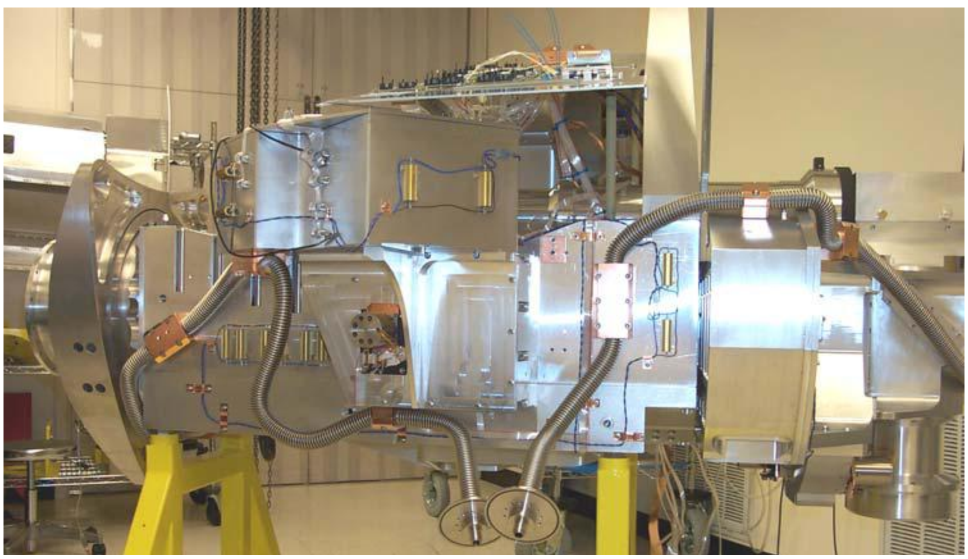

Figure 9. Optical bench assembled in the laboratory. Note the pre-cool tubing, including the dewar fittings. Several of the heater resistors are also visible. A section of the active shield is attached at the top; note the thermal isolation from the bench. This section of the shield also holds a “patch panel” for the dewar internal wiring. Note the Invar collars used to compensate for differential thermal contraction of the bolts used in assembling the bench (four of these are visible along the top of the bench, at the end on the left).

Figure 9 also shows the design for compensation for the differential thermal contraction of the optical bench structure (Al 6061) and the bolts used in assembling it (typically 300-series stainless). Without compensation, the bench would shrink when cooled by a significant amount relative to the bolts. In order to compensate for this effect, an Invar collar is used between the bolt head and the bench, so that the net contraction of bench plus collar from room temperature to 60 K is equal to the contraction of the bolt.

This same design was used for all structurally critical bolts and for bolted joints in the cooling path.

ACKNOWLEDGEMENTS

The National Optical Astronomy Observatory is operated by the Association of Universities for Research in Astronomy, Inc. (AURA) under cooperative agreement with the National Science Foundation.

The Gemini Observatory is operated by the Association of Universities for Research in Astronomy, Inc., under a cooperative agreement with the NSF on behalf of the Gemini partnership: the National Science Foundation (United States), the Particle Physics and Astronomy Research Council (United Kingdom), the National Research Council (Canada), CONICYT (Chile), the Australian Research Council (Australia), CNPq (Brazil), and CONICET (Argentina).

This instrument could not have constructed without the work of a very large number of people, at NOAO, Gemini, and elsewhere; we are grateful to all of them for their assistance. We would like to single out the GNIRS Project Manager, Neil Gaughan, for his leadership of the project, and NOAO Directors Sidney Wolff and Jeremy Mould for their support over the life of the project.

REFERENCES

1. Mountain, M., "A Scientific Perspective on the Requirements for the 1-5 Micron Spectrograph," *Gemini Technical Note* TN-PS-G0020 (1994).
2. J. H. Elias, B. Rodgers, R. R. Joyce, M. Lazo, G. Doppmann, C. Winge, and A. Ardila, "Performance of the Gemini near-infrared spectrograph", *Proc. SPIE* 6269-41 (2006).
3. B. Gregory, J. Elias, R. Elston, and T. Ellis, "Design of an efficient infrared spectrometer for large telescopes," *Proc. SPIE* 2475, 318 (1995).
4. J. H. Elias, D. Vukobratovich, J. R. Andrew, M. K. Myung K.; R. W. Cuberly, K. Don, A. Gerzoff, C. F. Harmer, D. Harris, J. B. Heynssens, J. Hicks, A. Kovacs, C. Li, M. Liang, I. K. Moon, E. T. Pearson, G. Plum, N. A. Roddier, J. Tvedt, R. J. Wolff, and W.-Y. Wong, "Design of the Gemini near-infrared spectrometer," *Proc. SPIE* Vol. 3354, 555 (1998).
5. K. W. Hodapp, J. B. Jensen, E. M. Irwin, H. Yamada, R. Chung, K. Fletcher, L. Robertson, J. L. Hora, D. A. Simons, W. Mays, R. Nolan, M. Bec, M. Merrill, and A. M. Fowler, "The Gemini Near-Infrared Imager (NIRI)," *PASP* 115, 1388 (2003).
6. W. Harrison, A. M. Fowler, and W. Ball, "Characterization of Gemini near-IR arrays," *Proc. SPIE* 3354, p. 214 (1998).
7. K.-W. Hodapp, E. M. Irwin, H. Yamada, R. Chung, K. Fletcher, J. Jensen, W. Mays, R. Nolan, D. A. Simons, and C. Aspin, "Gemini near-infrared imager (NIRI): a discussion of its design features and performance," *Proc. SPIE* 4841, 869 (2003).
8. K. A. Snail, D. P. Brown, J. P. Costantino, W. C. Shemano, C. W. Schmidt, W. F. Lynn, C. L. Seaman, and T. R. Knowles, "Optical characterization of black appliques," *Proc. SPIE* 2864, 465 (1996).
9. D. Vukobratovich, K. Don, and R. E. Sumner, "Improved cryogenic aluminum mirrors," *Proc. SPIE* 3435, 9 (1998).
10. M. Dubbeldam, R. Content, J. R. Allington-Smith, S. Pokrovki, and D. J. Robertson, "Integral field unit for the Gemini near-infrared spectrograph," *Proc. SPIE* 4008, 1181 (2000).
11. J. R. Allington-Smith, C. M. Dubbeldam, R. Content, C. J. Dunlop, D. J. Robertson, J. Elias, B. Rodgers, and J. E. Turner, "Integral field spectroscopy with the Gemini Near-Infrared Spectrograph," *Proc. SPIE* 5492, 701 (2004).
12. E. A. Hileman, J. Elias, R. Joyce, R. Probst, M. Liang, and E. Pearson, "Passive compensation of gravity flexure in optical instruments," *Proc. SPIE* 5495, 622 (2004).